Isothermal self-assembly of multicomponent and evolutive DNA nanostructures

Caroline Rossi-Gendron,[1,$] Farah El Fakih,[1,$] Koyomi Nakazawa,[1] Léa Chocron, [1] Masayuki Endo,[2,3] Hiroshi Sugiyama,[2,4] Mathieu Morel, [1] Sergii Rudiuk, [1] and Damien Baigl[1,*]

[1] PASTEUR, Department of Chemistry, École Normale Supérieure, PSL University, Sorbonne Université, CNRS, 75005 Paris, France

[2] Department of Chemistry, Graduate School of Science, Kyoto University, Kitashirakawa-Oiwakecho, Sakyo-Ku, Kyoto 606-8502, Japan

[3] Organization for Research and Development of Innovative Science and Technology, Kansai University, Suita, Osaka 564-8680, Japan

[4] Institute for Integrated Cell-Material Sciences (WPI-iCeMS), Kyoto University, Yoshida-Ushinomaecho, Sakyo-Ku, Kyoto 606-8501, Japan

[$]: equal contribution

* correspondence to: damien.baigl@ens.psl.eu

Abstract

Self-assembly is both an advantageously spontaneous process to organize molecular or colloidal entities into synthetic functional superstructures and a key-feature of how life builds its components. However, compared to their living counterparts, synthetic materials made by self-assembly usually lack some of the interesting properties of living systems such as multicomponent character or capability to adapt, transform and evolve.[1] Here we describe an isothermal multicomponent DNA self-assembly method that recapitulates all these characteristics and leads to user-defined objects with programmable shape, site-specific function, intrinsic reconfigurability and unprecedented capacity of major transformation and shape evolution. Using a generic magnesium-free buffer containing NaCl, we show that a complex cocktail of hundreds of different DNA strands can spontaneously assemble at room or body temperature to form desired DNA origamis[2] of various shapes with site-specific protein functionalization, extended nanogrids[3] or single-strand tile-assemblies.[4] *In situ* atomic force microscopy allows us to follow the self-assembly process and demonstrate that DNA origami assembly proceeds through multiple folding pathways, the system escaping kinetic traps until it reaches its equilibrium target structure. We also show that, under thermodynamic control, this method allows a given system to self-select its most stable shape in a large pool of competitive DNA strands. We finally demonstrate the first giant morphological transformation of DNA origamis spontaneously evolving at constant temperature from one shape to a radically different one by the massive exchange of all its constitutive staple strands. This method greatly expands the repertoire of shapes and functions attainable by isothermal self-assembly as well as provides tools to design evolutive DNA assemblies, with applications ranging from directed or self-adaptive morphological changes to nanostructure optimization by evolution.

Introduction

Self-assembly denotes a process where individual bricks, such as molecules or colloids, embed the necessary information to spontaneously interact and self-organize into functional superstructures of interest.[1] Operator-free, it advantageously limits errors, intermediate steps and energy consumption, making it a particularly suitable approach for the construction of sustainable and smart materials. Synthetic materials made by self-assembly are usually equilibrium structures resulting from the spatial organization of a repeating single component into a stable structure, such as micelles or colloidal crystals, with a prescribed set of useful properties. They usually have however limited intrinsic reconfigurability and producing desired structures with more than a few different components is still highly challenging. In nature, self-assembled systems are key-elements of living entities and, contrary to their synthetic counterparts, are usually out-of-equilibrium and multicomponent structures capable of dynamic behaviors such as reconfigurability, adaptation or evolution. Obtaining multiple-component self-assembling synthetic materials capable of such life-like functions would arguably expand the applicability, versatility and sustainability of human-made materials. By exploiting the sequence-dependent base pairing principle between synthetic DNA single strands, and compatible with large-scale production,[5] DNA structural nanotechnology[6] appears as a particularly powerful approach to address this challenge, as it allows to program the assembly of hundreds of different components into elaborate superstructures of desired shape,[2,4] size[7,8] and site-specific functionality,[2,9] leading to a large scope of applications.[10,11] The flawless assembly of such multicomponent structures is however usually ensured by a thermal annealing step where the DNA mixture is first heated above its melting temperature before being slowly cooled down to avoid kinetic traps and ensure proper sequence-specific DNA hybridization.[12] Such a thermal treatment hinders any possibility for spontaneous nanostructure formation or evolution under fixed environmental conditions. This also leads to energetically highly stabilized structures for which dynamic actuation and transformation is possible,[13–17] but typically relies on supplemental action on preformed objects,[18] using for instance linker strand hybridization,[19–21] strand-displacement,[22] supramolecular interactions,[23] enzymatic editing,[24] or photo-actuation strategies.[25,26] Thermal annealing thus produces structures that can be actuated once they are formed but that are not intrinsically evolutive. It also constitutes an obstacle to one-pot, *in situ* functionalization with temperature-sensitive entities such as proteins. From a more fundamental viewpoint, it also raises the question whether such sophisticated, multicomponent DNA nanostructures could self-assemble without mistake at constant temperature. A few isothermal protocols have been described in literature but all having some specific limitations such as involving denaturing agents,[27–29] preformed assemblies,[30] specific sequence designs[31] or working temperatures.[32,33] Most of the isothermal approaches were also dedicated to a specific DNA assembly method (e.g. DNA origami or single-stranded tile (SST) assembly), lacking a generic character that could benefit for increased applicability and better understanding of DNA isothermal self-assembly. In this work, we show that the major methods of structural DNA nanotechnology, including DNA origamis,[2] DNA nanogrids[3] and SST assemblies,[4] can now be operated by the same generic isothermal DNA self-assembly principle, leading to a breadth of user-defined elaborate DNA nanostructures that can be spontaneously formed at room or body temperature, keeping intrinsic reconfigurability and a capability of massive transformation never achieved so far. By using a magnesium-free buffer containing NaCl to electrostatically stabilize the forming structures while allowing enough reconfigurability, we established the range of temperatures and salt concentrations where the

self-assembly was operational and applied it to the isothermal production of various nanostructure designs and shapes as well as their concomitant functionalization by proteins. By *in situ* real-time atomic force microscopy (AFM), we revealed the multiplicity of folding pathways in self-assembling origamis. Finally, we performed a series of experiments demonstrating some unique characteristics of this thermodynamically controlled isothermal assembly method, ranging from shape selection in a highly-multicomponent mixture of competing DNA strands to giant shape transformation by the massive exchange of hundreds of different strand components.

Results and discussion

First, we simply assembled a DNA origami mix (M13 scaffold + set of staples coding for sharp triangles), without any thermal pretreatment, and let it incubate at 25°C for several hours (Fig. 1A). When this was done in the conventionally used buffer (Trizma-base 40 mM, acetic acid 20 mM, $MgCl_2$ 12.5 mM), with or without EDTA, we did not observe any properly shaped objects, regardless of the incubation time (Fig. S1, *left* and *middle*), in agreement with a previous report.[27] We attribute this effect to the formation of kinetically trapped structures, for which the magnesium-stabilized base pairing would require a much higher thermal energy to allow structure reconfigurability.[34] We thus opted for an alternative buffer, referred to as TANa buffer, which was solely composed of tris-acetate buffer (Trizma-base 40 mM, acetic acid 20 mM), without EDTA nor magnesium to promote staple exchange and reconfiguration. It was supplemented instead with a monovalent salt (NaCl) to ensure enough electrostatic screening between the repulsive anionic DNA strands. Remarkably, with [NaCl] = 100 mM (Debye length λ_D = 0.8 nm) , we observed the progressive formation of properly folded triangles in a few hours at 25 °C (Fig. 1B). After 24 hours, the yield was comparable to that with thermal annealing operating in the same buffer (Fig. S2) and the resulting structures were stable over several days (Fig. S1, *right*). We repeated the isothermal procedure with the same origami mix in TANa buffer but for various fixed temperatures and NaCl concentrations. For each condition, we systematically established the ratio of mis-/unfolded (no triangular shape), partially folded (defined as incomplete triangular shapes with at least one well-formed corner) and fully folded (defined as triangles with three well-formed corners) origamis obtained after 24 h of self-assembly (Fig. 1C). Without or with a high amount (500 mM) of NaCl, we could not detect any properly folded origamis for all the tested temperatures. In contrast, for intermediate concentrations ranging from [NaCl] = 50 mM to 250 mM, a significant fraction of partially or fully folded origamis was obtained for different temperatures between 15 °C and 60 °C (Fig. 1C, Fig. S3, Table S1). Sufficient electrostatic screening was thus necessary to allow base pairing between anionic DNA strands but should not be too high to maintain some electrostatic repulsion at short distance and hamper the formation of mismatched assemblies. In this NaCl concentration range, origamis properly assembled up to a temperature increasing from 35 °C to 60 °C when NaCl increased from 50 mM to 250 mM, which was attributed to the electrostatic stabilization by salts against DNA melting. This led to a broad range of temperatures and NaCl concentrations for which isothermal self-assembly led to properly folded origamis after 24 h of incubation (Fig. 1C). It was found to be particularly efficient for [NaCl] = 100 – 150 mM, for which a majority of fully folded origamis was obtained when the assembly temperature was set in the range 25 – 40 °C with [NaCl] = 100 mM and 15 – 55 °C with [NaCl] = 150 mM (Figures S4-S6). We found that this was not specific to the triangle origami shape, as simply changing

the initial staple composition allowed us to successfully produce origamis of other target shapes, such as rectangles without staple edges to avoid inter-origami stacking or smileys, by isothermal self-assembly at 25 °C (Figures S7). Close-up AFM analysis revealed that, although the resulting origamis were not perfectly flawless, their overall shape and internal organization showed excellent similarity with the target structure (Figure 1D) and were comparable to what can be obtained with conventional thermal annealing (Figure S2). All these results demonstrate that isothermal self-assembly in TANa buffer allows one to generate well-defined and stable origamis of target morphology in several hours, in a broad window of working temperatures including room and body temperature.

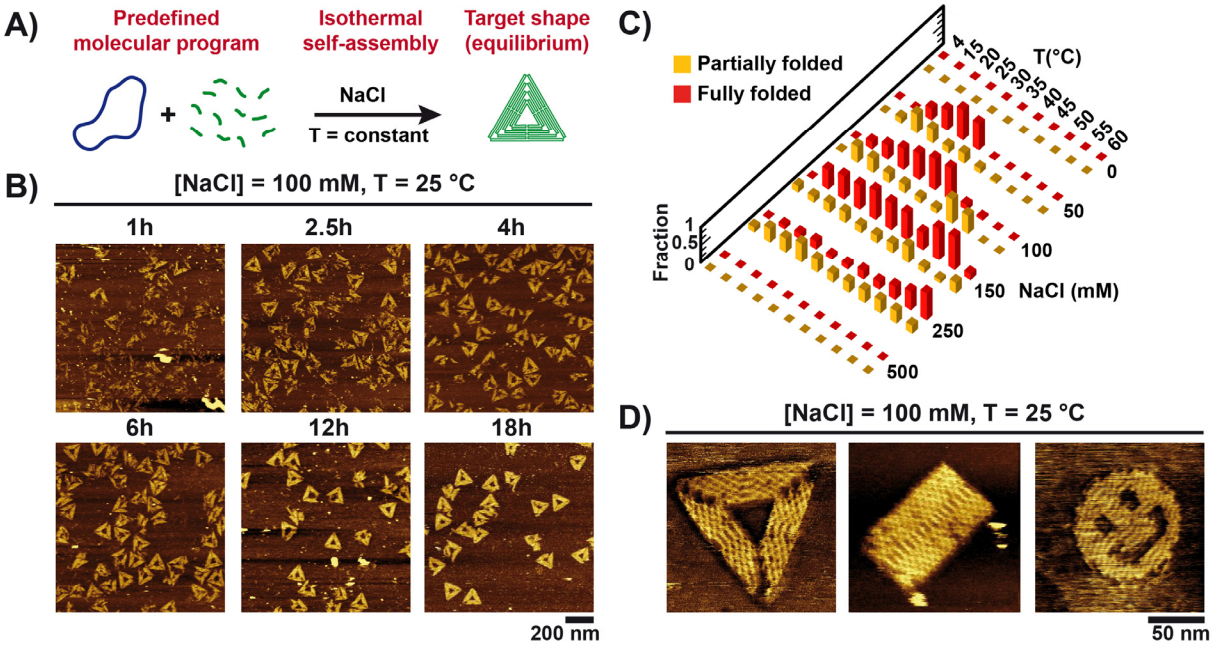

Figure 1. Isothermal self-assembly of user-defined DNA origamis in a magnesium-free NaCl buffer. A) An origami mix (M13 scaffold + set of desired staples) can spontaneously self-assemble at constant temperature into the target equilibrium shape (e.g., a triangle) in a buffer simply composed of tris-acetate 1× and NaCl, referred to as TANa buffer. B) Atomic force microscopy (AFM) observation of the isothermal origami formation at 25 °C in TANa ([NaCl] = 100 mM), for a set of staples coding for sharp triangles, as a function of incubation time. C) Fraction (vertical axis) of partially (yellow) and fully (red) folded origamis after 24 hours of isothermal self-assembly with a set of staples coding for sharp triangles, for various incubation temperatures (*T*) and NaCl concentrations. For the sake of readability, the remaining fraction of each histogram, which corresponds to non- or misfolded origamis, is not plotted in this graph but is displayed in Fig. S3 and Table S1. D) Representative close-up AFM images of origamis obtained by isothermal assembly in TANa ([NaCl] = 100 mM) at 25 °C for staples coding for sharp triangles (left), tall rectangles (middle) and smileys (right). For all experiments: [M13] = 1 nM; each staple concentration is 40 nM.

We then explored the applicability of our method to generate complex assemblies of various functionality, nature, shapes and sizes, by isothermal self-assembly at 25 °C in the TANa buffer. First, we achieved spatial control over the assembly progress by successfully programming the stepwise assembly of origamis by successive addition of different fractions of the staple set in the self-assembling mixture. This allowed us, for instance, to construct triangles either from a corner to the opposite edge or from an edge to the opposite corner (Fig. S8). Then, we targeted the preparation of protein-functionalized origamis. To this end, we directly mixed the M13 scaffold, staples coding for triangles and streptavidin as a model protein, and let the system

self-assemble at 25 °C for 24 h. We replaced the staples in the initial mix with up to 6 biotinylated ones to direct the streptavidin binding during the isothermal self-assembly and analyzed the localization of tethered streptavidin in the obtained origamis (Figs. 2A, S9). In the case of single-site functionalization, we found that 93% of available biotin sites were occupied by a streptavidin (Fig. S10) and all the bound streptavidin proteins were at the prescribed position (Fig. 2A, *left*). For multiple site functionalization, this occupation rate was slightly lower with 65, 70 and 71% of available sites occupied when we prepared origamis with 2, 3 and 6 binding sites, respectively (Fig. S10), but the large majority of detected proteins were bound to the origamis at the prescribed positions (Fig. 2A, *middle* and *right*). Isothermal self-assembly was thus shown to be perfectly compatible with *in situ* site-specific protein functionalization, offering new solutions for the self-assembly of functional hybrid DNA-protein structures involving in particular temperature-sensitive entities. With origamis, the large excess of staples with respect to the DNA scaffold favored the folding into the desired shape at a high yield. We thus challenged the possibility to prepare another kind of user-defined but scaffold-free DNA nanostructure. We chose the single-stranded tile (SST) technology, in which stoichiometric arrangement of the DNA strands leads to much lower yield but allows one to reach a large variety of shapes by simply removing strands from the same initial mix.[4] We thus simply prepared the SST mix of the so-called R4 rectangle in the TANa buffer and let it self-assemble at 25 °C. We followed the evolution of the system by AFM. After a few hours, we observed the formation of the first fully assembled R4 rectangles coexisting with a large number of ill-defined objects. The fraction of fully folded R4 rectangles increased slowly but substantially with time (Fig. 2B, *middle*), as confirmed by a characteristic band of increasing intensity observed by gel electrophoresis (Fig. 2B, *bottom left*). The purification of this band led to well-defined R4 rectangles (Fig. 2B, *bottom right*), demonstrating successful isothermal self-assembly at 25 °C of this reference SST system. Finally, to prepare objects of extended dimensions, we mixed 9 DNA strands that could organize in self-repeating units of an extended nanogrid, and let the system self-assemble at 25 °C in the TANa buffer. After 24 h of assembly, nanogrids of large dimensions were successfully obtained in the presence of NaCl, with a particularly sharp square motif at [NaCl] = 150 mM (Figs. 2C, S11). By allowing programmable DNA self-assembly at room temperature in systems of drastically different nature and composition (protein-modified origamis, well-folded SST structures, nanogrids), the isothermal self-assembly principle thus appears as a tool of remarkable robustness and versatility.

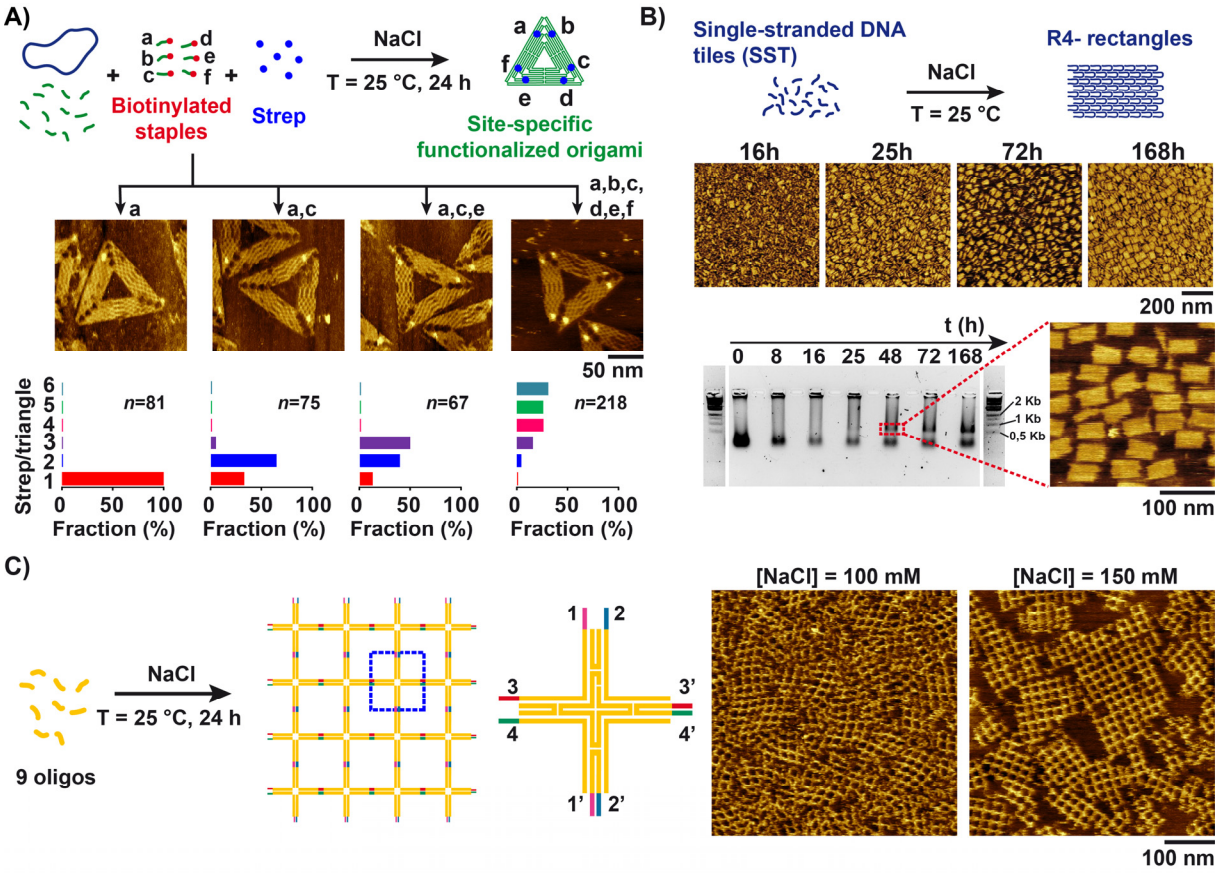

Figure 2. Expended applicability of the isothermal self-assembly: protein functionalization, tile assembly and nanogrid formation at 25 °C in TANa buffer. A) *Top*: Self-assembly of an origami mix with staples coding for sharp triangles, including biotinylated staples at specific position (named a to e), in the presence of streptavidin (Strep). *Middle*: Representative AFM images of the obtained origamis after 24 h of assembly in TANa ([NaCl] =100 mM), as a function of the biotinylated staples used in the mix. Larger-scale images are given in Fig. S9. *Bottom*: Fraction (%) of streptavidin detected on origamis functionalized with 1 to 6 streptavidin. *n* is the number of analyzed objects. [M13] = 1 nM; each staple concentration is 40 nM. B) *Top* : Self-assembly of DNA strands called single-strand tiles (SST) into a R4 rectangle with 100 mM NaCl. *Middle*: AFM images as a function of self-assembly time. *Bottom*: Electrophoresis gel of the self-assembling mixture as a function of time, with ladders shown in extreme left and right. On the right, AFM image of R4 rectangle after extraction and purification of the band shown on the left. C) Self-assembly of 9 oligonuclotides (1 µM each) forming extended DNA nanogrids with representative AFM images after 24 h assembly with [NaCl] =100 mM (left) or 150 mM (right). Larger-scale images are given in Fig. S11.

To characterize the mechanism of the isothermal self-assembly, we devised a method to follow *in situ* and in real time the folding pathway of DNA origamis. To keep most of the dynamic features possible upon surface adsorption for AFM imaging, we used a mica substrate coated by a supported lipid bilayer. It was shown in previous works that origamis could adsorb on such substrates through electrostatic interactions mediated by magnesium ions and keep their mobility once adsorbed.[35] To avoid the presence of magnesium ions, we chose another adsorption method by using a few cholesterol-modified staples to anchor parts of the origamis to the bilayer-coated surface. We prepared Λ-shaped origamis by thermal annealing in the TANa buffer by using an origami mix for a triangular shape with cholesterol modifications on two of the sides but depleted from the staples of the third side (Fig. S12), and absorbed them on the lipid bilayer. Each adsorbed object was therefore composed of two anchored folded sides

and an unfolded, unmodified single-stranded M13 fragment with no prescribed folding constrain and minimal interactions with the surface. This system was then maintained at 25 °C in the TANa buffer containing unadsorbed Λ structures and their excess of staples. We added to this solution the staples of the triangle missing side and followed *in situ* and in real time the folding of the M13 fragment (Movie S1). At $t = 0$ (addition of staples), all adsorbed objects had the characteristic Λ shape. Strikingly, with increasing time, we observed that some of the adsorbed structures evolved to form well-defined triangular origamis, indicating complete folding of the M13 fragment into a perfectly arranged triangle side (Fig. 3A, white circles). Contrary to experiments performed so far allowing to make snapshots at a given time of a population of origamis,[36] here we provide the whole temporal evolution of individual structures from an unfolded M13 fragment to the folded state at equilibrium. Notably, several fully folded triangles adsorbed in the field of view during imaging, indicating that isothermal folding also occurred in bulk and at a higher speed than on the surface (Fig. 3A, blue circle). Incompletely folded entities also adsorbed and tended to continue their folding process once adsorbed (Fig. 3A, yellow circle). A detailed look at the initially adsorbed origamis evolving to fully folded structures revealed that individual origamis followed markedly different pathways (Figs 3B-E). One observed pathway consisted in a folding process nucleating at one triangle corner, *i.e.*, an extremity of the free M13 fragment, and progressing toward the opposite extremity (Fig. 3B, movie S2), a mechanism reminiscent to the DNA assembly nucleation-growth process in SST revealed in the past by computer simulation.[37] Folding parallel to the triangle edge was also observed in two different directions, either from the inside to the outside (Fig. 3C, movie S3) or from the outside to the inside (Fig. 3D, movie S4). These observations reveal that attaining the equilibrium structure for an individual origami is not constrained to one specific folding pathway[38] but to multiple ones (Fig. 3E). The apparent diversity of these evolutions emphasizes that, contrary to experiments in a magnesium-containing buffer (Fig. S1), the system in TANa buffer is not kinetically trapped. We thus conclude that isothermal origami formation in our conditions is a thermodynamically controlled process where the equilibrium state constituted by properly folded origamis can be spontaneously reached by self-assembly.

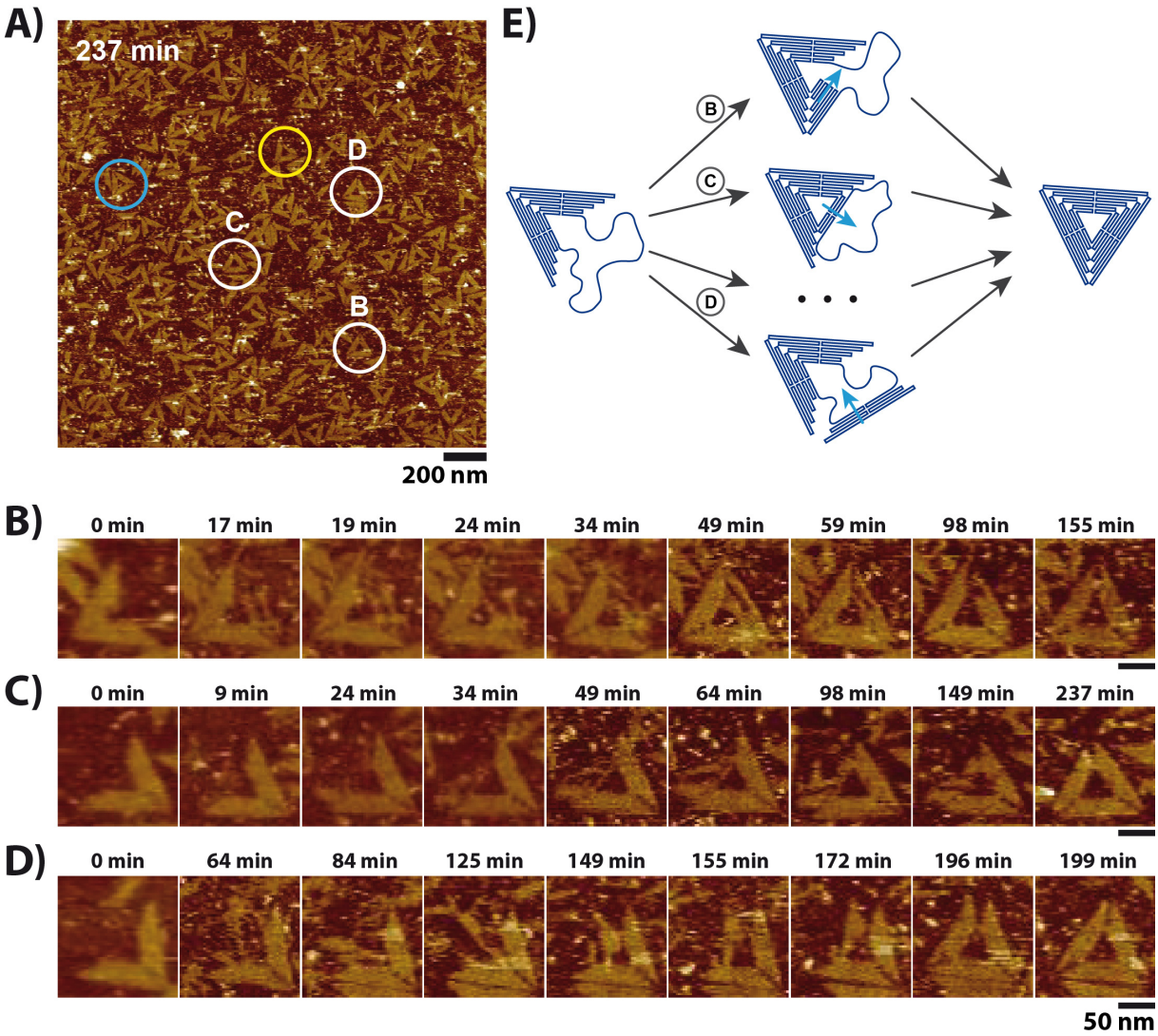

Figure 3. ***In situ*** **visualization of the isothermal folding reveals the multiple folding pathways of a process under thermodynamic control**. A) Cholesterol-modified Λ-shaped origamis were initially adsorbed on a supported lipid bilayer and carried an unfolded M13 fragment to be folded into a third triangle side. The image is a snapshot obtained after 237 min of real-time AFM observation at 25 °C in the TANa buffer ([NaCl] = 1 mM) supplemented with 1 mM EDTA, where $t = 0$ corresponds to the addition of staples programming the folding of the M13 fragment (see full movie S1). Circles indicate characteristic examples of i) complete origami folding from initially adsorbed state (white), ii) complete origami folding in bulk prior to adsorption (blue), iii) adsorption of origamis followed by folding (yellow). B-D) Detailed evolution of the folding process of the three individual origamis indicated by white circles in (A) evidencing three characteristic folding pathways from the initial Λ shape to the fully folded triangle. Images are extracted from Movies S2-S4. E) Schematic diagram showing at least three folding pathways. [M13] = 1 nM; each staple concentration is 40 nM.

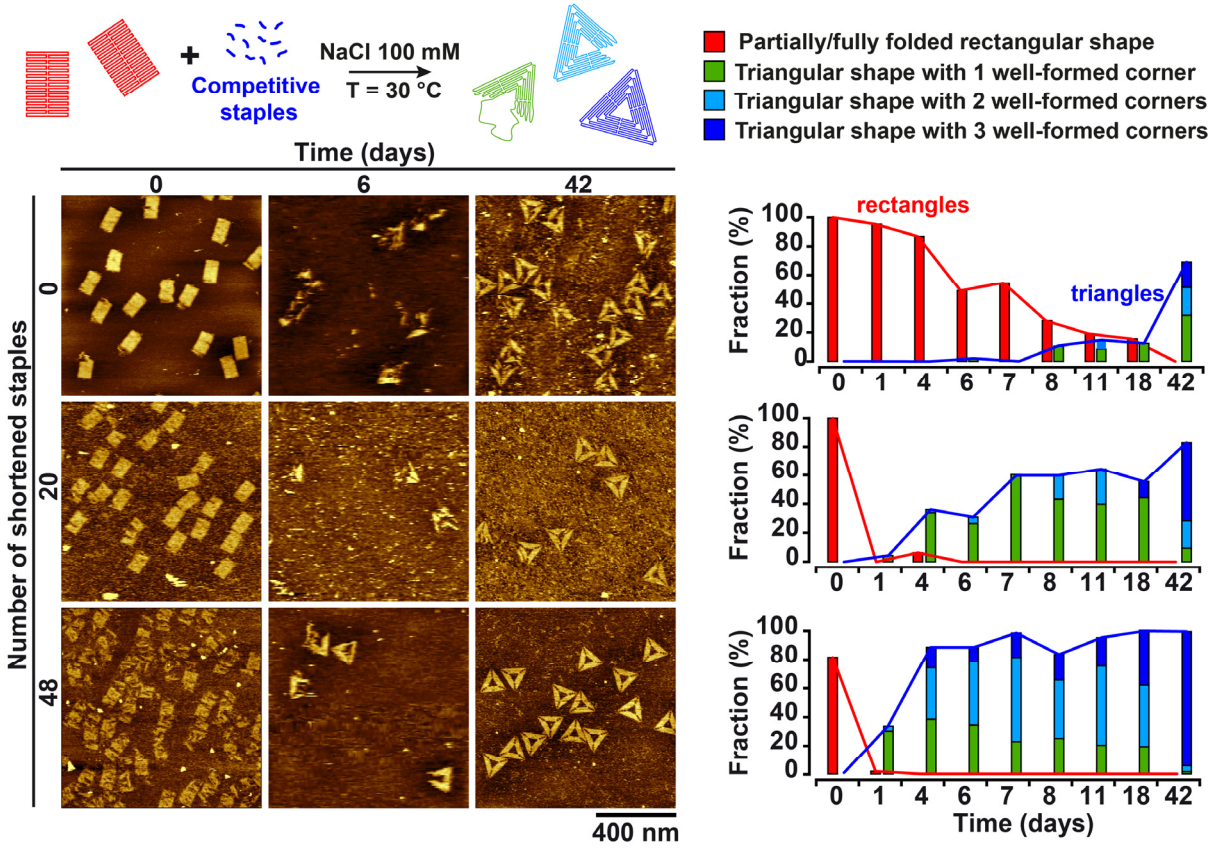

Figure 4. Evolution under thermal equilibrium: giant morphological transformation by massive strand displacement at constant temperature. *Top* : Schematic principle of the experiment: stable rectangle origamis are mixed with a 10-fold excess of a competitive set of staples coding for full triangles in the TANa buffer and progressively evolve into triangles at constant temperature (30 °C). *Bottom left:* Representative AFM images of the structures evolving in time when the initial set of staples for rectangles contained 0, 20 or 48 shortened staples (see Main Text and Materials and Methods for details). Bottom right: Fraction (color bar) of detected objects (number of analyzed objects in Table S2) with a partial or fully folded rectangular shape (red) or triangular shape with 1 (green), 2 (light blue) or 3 (dark blue) well-formed corners, after an increasing incubation time, with 0 (top), 20 (middle) or 48 (bottom) shortened staples in the rectangle. The remaining fraction of each histogram, which corresponds to mis-shaped or ill-defined objects, is not plotted in this graph. The bars for triangular shapes are shown in a stacked manner; the red and blue lines indicate the cumulative fraction of rectangular and triangular shapes, respectively. [M13] = 0.25 nM; each staple concentration is 10 nM (rectangle) or 100 nM (triangle).

With our method, DNA nanostructures spontaneously self-assembled at constant temperature and progressively evolved toward their equilibrium state by exploring multiple folding pathways through a complex free energy landscape without being kinetically trapped. To explore the applicability of such a unique thermodynamic control, we mixed the M13 scaffold with an equimolar mixture of two sets of staples coding for origami shapes of different stability, in this case triangles versus staple edge-free rectangles. Properly folding rectangle would lead to 1105 unpaired bases for 64 free ends, *i.e.*, double stranded helices that have no neighboring base pair and thus no stacking partner, while the triangle structures involved only 97 unpaired bases and 54 free ends. We could thus expect the triangle to be on a lower energetic level and therefore thermodynamically more stable since more bases of the scaffold are paired in the fully assembled state. We let the system evolve at 25 °C in TANa buffer ([NaCl] = 100 mM). Regardless of the incubation time, from a few minutes to several days, we did not detect any

rectangular shapes, neither partial or complete, nor any triangle-rectangle chimera. In contrast, we observed the progressive self-assembly of triangle origamis only (Fig. S13), showing that the system spontaneously evolved toward the lower free energy minimum and, as such, was capable to self-select its most stable state in a complex pool of multiple and competing components. We thus expect that chimera could appear but only when they correspond to a free energy minimum.[39] Then, we prepared rectangle origamis in TANa ([NaCl] = 100 mM) by thermal annealing, and exposed them without any purification, *i.e.*, keeping the rectangle staples in solution, to additional staples coding for sharp triangles and let the system evolve at a constant temperature (Fig. 4, *top row*). Remarkably, at 30 °C and with a 10-fold excess of triangle staples, rectangles disappeared in time to be progressively replaced with an increasing amount of triangular structures. This process was probably facilitated by the large amount of unpaired bases on the rectangle edges. With a concentration much lower than that of each staple, the M13 scaffold was the limited reagent in this system. We thus witnessed what appeared to be the first giant origami shape transformation by massive strand displacement of all of its constitutive staples. We further exploited this feature to tune the efficiency and speed of the transformation. To this end, we identified the staples in the rectangle structures binding by one extremity to a sequence of 8 consecutive bases of the scaffold sequence that was bound by a unique staple in the edges of the triangle structure (see Materials and Methods section for details). 48 staples of the rectangle were satisfying this criterion. We created shortened versions of these staples by removing the three first (5' side) or last (3' side) bases to these specific extremities, and repeated the isothermal transformation experiment using 20 or 48 shortened staples in the initial rectangle design. In this case (Fig. 4, *middle and bottom rows*), rectangles disappeared in one day only while it took over 40 days with full-length staples. This was accompanied by a faster formation of triangles at a rate increasing with an increase in the fraction of shortened staples, *i.e.*, increasing amounts of toeholds to initiate the formation of the triangle edges. With 48 shorter staples, the initial rectangles displayed a looser structure but the transformation was particularly efficient with 88.1 % of origamis having a triangular shape with at least one well-formed corner after 4 days of isothermal transformation. After 42 days, 93.4 % of the origamis were perfectly formed triangles. Using a higher salt concentration ([NaCl] = 150 mM) at 30 °C led to the stabilization of the initial rectangle structures and shortening the staples was necessary to observe significant transformation into triangles (Fig. S14). With [NaCl] = 100 mM but at 25 °C, rectangles slowly acquired a looser structure but did not transform into triangles within the 54 days of the experiment. Shortening the staples significantly improved the process and transformation from rectangle to well-formed triangles was observed in a few days with a kinetic and efficiency comparable to that at 30°C (Fig. S15, Table S3), while decreasing the triangle over rectangle staple ratio from 10 to 1 resulted in a much slower transformation, even in the presence of shortened staples (Fig. S16, Table S4). All these results demonstrated that our self-assembly method allowed one to achieve spontaneous evolution under thermal equilibrium from one origami shape to a dramatically different one when the system is exposed to a competitive set of staples leading to a thermodynamically more stable shape. Based on a multicomponent massive strand displacement process, the kinetic of this transformation was strongly dependent on the staple composition and could be accelerated and adjusted by increasing the ratio of competitive staples and creating toeholds in the initial shape.

Conclusion

We have reported for the first time that by using a generic magnesium-free saline buffer, simply composed of tris-acetate buffer supplemented by a suitable concentration of NaCl, highly multicomponent mixtures of DNA strands spontaneously self-assembled at room temperature and isothermally evolved toward their equilibrium state consisting in properly shaped objects. We demonstrated that this isothermal self-assembly could be operated in a broad range of temperatures (15 – 60 °C) and salt concentrations (50 – 250 mM), and was compatible with various designs that could be either scaffolded (origamis of different shapes) or scaffold-free (SST assemblies, DNA nanogrids), producing highly multicomponent motifs of well-defined size and shapes (origamis, SST) or self-repeating units extending in space (DNA nanogrids), while allowing *in situ* site-specific functionalization by proteins. With such a versatile and robust character, this isothermal self-assembly method is not only a novel and user-friendly way to produce functional nanostructures but also holds great perspectives to be combined with more sophisticated designs to generate tridimensional structures[8,40] and/or larger-scale assemblies.[7] Contrarily to conventional thermal annealing-based procedures, this isothermal self-assembly process was shown to be thermodynamically driven. With a buffer allowing reconfigurability and folding/assembly pathway exploration, kinetic traps were avoided and isothermal conditions let the DNA mixture progressively evolve until reaching the most stable state defined by the properly assembled nanostructure. This feature opens up new horizons for autonomous structure selection and evolution in competitive systems. For instance, we demonstrated here that a complex mixture of competitive DNA strands coding simultaneously for different shapes led to the successful and selective formation of the most stable shape only, thermodynamically unfavored competitive shapes, chimera or mis-folded structures being avoided. Demonstrated here with only two different competing shapes, it would be interesting to explore more complex mixtures, either to test models with designed strand mixes[38,39] or to discover new set of DNA strands producing structures with better shape or functionality, for example to recognize and/or capture a target protein[41,42] added to the self-assembling strands. Finally, we showed that this competitive selection capability was not restricted to a mixture of initially unbound DNA strands but was also effective starting from preformed assemblies to produce new dynamic responses. We demonstrated in particular that preformed DNA origamis exposed to a full set of competitive staples could spontaneously evolve and transform into a radically different shape by the exchange of all its constitutive DNA staples through a massive strand-displacement reaction. Thermodynamically driven and adjustable through staple composition and temperature, this process allows for complex DNA assemblies to morphologically evolve each time a new free energy minimum appears, for instance in response to a change in their composition or environment. This constitutes a novel and valuable route to build smart nanomachines capable to morphologically evolve with an encoded predefined dynamics or self-adapting to a changing environment. This opens particularly interesting perspectives for dynamic operations in living systems where the temperature is fixed, as well as for nanostructure discovery by directed evolution-inspired protocols where improved structures of complex shapes (e.g., protein binder) could emerge and be selected from large libraries of DNA components.

Funding

This work was supported by the European Research Council (ERC) (European Community's Seventh Framework Programme (FP7/2007−2013)/ERC Grant Agreement No. 258782, to D.B.), the French National Research Agency ANR contracts DYOR (ANR-18-CE06-0019, to D.B.) and ActiveGEL (ANR-18-CE07-0001, to S.R.), a grant from the graduate school "Chimie Physique et Chimie Analytique de Paris-Centre (ED388)" to C.R.G., an Overseas Research Fellowship from the Japan Society for the Promotion of Science (JSPS) to K.N., and a JSPS Summer Program grant to C.R.G.

Acknowledgement

We thank A. Estevez-Torres (Sorbonne Université), J. Lee Tin Wah (Sorbonne Université), L. Nurdin (Ecole Normale Supérieure) and V. Jallet (Ecole Normale Supérieure) for contributions in developing the DNA origami technology in the laboratory; R. Barbattini and J. Lopez (Oxford Instruments) for crucial support in the implementation of Cypher ES AFM instrument; K. Hidaka, T. Emura and Y. Kamada (Kyoto University) for instrumental and technical support; P. Sulc (Arizona State University), R. Kosinki (Universität Duisburg-Essen) and B. Saccà (Universität Duisburg-Essen) for insightful discussions.

Conflict of interest

The authors declare no conflict of interest.

Author contribution

C.R.G. developed the isothermal self-assembly principle; C.R.G. and F.E.F performed and analyzed most of the experiments: AFM imaging optimization (C.R.G. and F.E.F.), isothermal assembly of DNA origamis at room temperature (C.R.G) and other experimental conditions (F.E.F.), stepwise assembly (F.E.F.), protein functionalization (F.E.F.), nanogrid assembly (F.E.F.), multiple folding pathway characterization (C.R.G.), competition and transformation (C.R.G. and F.E.F.); K.N. performed the self-assembly of SST R4-rectangles; L.C. contributed to isothermal self-assembly and protein functionalization experiments; M.E. and H.S. supervised the multiple folding pathway characterization; M.M. and S.R. contributed to the overall supervision; all authors contributed to data analysis and manuscript writing and edition; D.B. supervised the entire work and wrote the paper.

References

1. Whitesides, G. M. & Grzybowski, B. Self-assembly at all scales. *Science* **295**, 2418–2421 (2002).
2. Rothemund, P. W. K. Folding DNA to create nanoscale shapes and patterns. *Nature* **440**, 297–302 (2006).
3. Yan, H., Park, S. H., Finkelstein, G., Reif, J. H. & LaBean, T. H. DNA-Templated

Self-Assembly of Protein Arrays and Highly Conductive Nanowires. *Science* **301**, 1882–1884 (2003).

4. Wei, B., Dai, M. & Yin, P. Complex shapes self-assembled from single-stranded DNA tiles. *Nature* **485**, 623–626 (2012).

5. Praetorius, F. *et al.* Biotechnological mass production of DNA origami. *Nature* **552**, 84–87 (2017).

6. Seeman, N. C. Nucleic acid junctions and lattices. *J. Theor. Biol.* **99**, 237–247 (1982).

7. Wagenbauer, K. F., Sigl, C. & Dietz, H. Gigadalton-scale shape-programmable DNA assemblies. *Nature* **552**, 78–83 (2017).

8. Ong, L. L. *et al.* Programmable self-assembly of three-dimensional nanostructures from 10,000 unique components. *Nature* **552**, 72–77 (2017).

9. Saccà, B. *et al.* Orthogonal protein decoration of DNA origami. *Angew. Chemie - Int. Ed.* **49**, 9378–9383 (2010).

10. Seeman, N. C. & Sleiman, H. F. DNA nanotechnology. *Nat. Rev. Mater.* **3**, 17068 (2018).

11. Hong, F., Zhang, F., Liu, Y. & Yan, H. DNA Origami: Scaffolds for Creating Higher Order Structures. *Chem. Rev.* **117**, 12584–12640 (2017).

12. Lee Tin Wah, J., David, C., Rudiuk, S., Baigl, D. & Estevez-Torres, A. Observing and Controlling the Folding Pathway of DNA Origami at the Nanoscale. *ACS Nano* acsnano.5b05972 (2016). doi:10.1021/acsnano.5b05972

13. Andersen, E. S. *et al.* Self-assembly of a nanoscale DNA box with a controllable lid. *Nature* **459**, 73–76 (2009).

14. Gerling, T., Wagenbauer, K. F., Neuner, A. M. & Dietz, H. Dynamic DNA devices and assemblies formed by shape-complementary, non–base pairing 3D components. *Science* **347**, 1446–1452 (2015).

15. Engelen, W., Sigl, C., Kadletz, K., Willner, E. M. & Dietz, H. Antigen-Triggered Logic-Gating of DNA Nanodevices. *J. Am. Chem. Soc.* **143**, 21630–21636 (2021).

16. Wang, D. *et al.* Programming the Curvatures in Reconfigurable DNA Domino Origami by Using Asymmetric Units. *Nano Lett.* **20**, 8236–8241 (2020).

17. Wang, D. *et al.* Programmable Transformations of DNA Origami Made of Small Modular Dynamic Units. *J. Am. Chem. Soc.* **143**, 2256–2263 (2021).

18. Daljit Singh, J. K., Luu, M. T., Abbas, A. & Wickham, S. F. J. Switchable DNA-origami nanostructures that respond to their environment and their applications. *Biophys. Rev.* **10**, 1283–1293 (2018).

19. Chen, H. *et al.* Understanding the mechanical properties of DNA origami tiles and controlling the kinetics of their folding and unfolding reconfiguration. *J. Am. Chem. Soc.* **136**, 6995–7005 (2014).

20. Liu, Y. *et al.* Modular Reconfigurable DNA Origami: From Two-Dimensional to Three-Dimensional Structures. *Angew. Chemie - Int. Ed.* **59**, 23277–23282 (2020).

21. Suzuki, Y., Kawamata, I., Mizuno, K. & Murata, S. Large Deformation of a DNA-

Origami Nanoarm Induced by the Cumulative Actuation of Tension-Adjustable Modules. *Angew. Chemie Int. Ed.* **59**, 6230–6234 (2020).

22. Yurke, B., Turberfield, A. J., Mills, A. P., Simmel, F. C. & Neumann, J. L. A DNA-fuelled molecular machine made of DNA. *Nature* **406**, 605–608 (2000).

23. Nakazawa, K. *et al.* Reversible Supra-Folding of User-Programmed Functional DNA Nanostructures on Fuzzy Cationic Substrates. *Angew. Chemie Int. Ed.* **60**, 15214–15219 (2021).

24. Xiong, Q. *et al.* DNA Origami Post-Processing by CRISPR-Cas12a. *Angew. Chemie Int. Ed.* **59**, 3956–3960 (2020).

25. Endo, M. *et al.* Single-Molecule Observation of The Photoregulated Conformational Dynamics of DNA Origami Nanoscissors. *Angew. Chemie Int. Ed.* (2017). doi:10.1002/anie.201708722

26. Chen, H., Li, R., Li, S., Andreásson, J. & Choi, J. H. Conformational effects of UV light on DNA origami. *J. Am. Chem. Soc.* **139**, 1380–1383 (2017).

27. Jungmann, R., Liedl, T., Sobey, T. L., Shih, W. & Simmel, F. C. Isothermal Assembly of DNA Origami Structures Using Denaturing Agents. *J. Am. Chem. Soc.* **130**, 10062–10063 (2008).

28. Zhang, Z., Song, J., Besenbacher, F., Dong, M. & Gothelf, K. V. Self-Assembly of DNA Origami and Single-Stranded Tile Structures at Room Temperature. *Angew. Chemie Int. Ed.* **52**, 9219–9223 (2013).

29. Kopielski, A., Schneider, A., Csáki, A. & Fritzsche, W. Isothermal DNA origami folding: avoiding denaturing conditions for one-pot, hybrid-component annealing. *Nanoscale* **7**, 2102–2106 (2015).

30. Song, J. *et al.* Isothermal Hybridization Kinetics of DNA Assembly of Two-Dimensional DNA Origami. *Small* **9**, 2954–2959 (2013).

31. Myhrvold, C., Dai, M., Silver, P. A. & Yin, P. Isothermal Self-Assembly of Complex DNA Structures under Diverse and Biocompatible Conditions. *Nano Lett.* **13**, 4242–4248 (2013).

32. Sobczak, J.-P. J., Martin, T. G., Gerling, T. & Dietz, H. Rapid Folding of DNA into Nanoscale Shapes at Constant Temperature. *Science* **338**, 1458–1461 (2012).

33. Song, J. *et al.* Reconfiguration of DNA molecular arrays driven by information relay. *Science* **357**, 1–13 (2017).

34. Martin, T. G. & Dietz, H. Magnesium-free self-assembly of multi-layer DNA objects. *Nat. Commun.* **3**, 1103 (2012).

35. Suzuki, Y., Endo, M. & Sugiyama, H. Lipid-bilayer-assisted two-dimensional self-assembly of DNA origami nanostructures. *Nat. Commun.* **6**, 8052 (2015).

36. Lee Tin Wah, J., David, C., Rudiuk, S., Baigl, D. & Estevez-Torres, A. Observing and Controlling the Folding Pathway of DNA Origami at the Nanoscale. *ACS Nano* **10**, 1978–1987 (2016).

37. Reinhardt, A. & Frenkel, D. Numerical Evidence for Nucleated Self-Assembly of DNA Brick Structures. *Phys. Rev. Lett.* **112**, 238103 (2014).

38. Dunn, K. E. *et al.* Guiding the folding pathway of DNA origami. *Nature* **525**, 82–86 (2015).

39. Majikes, J. M., Nash, J. A. & LaBean, T. H. Competitive annealing of multiple DNA origami: formation of chimeric origami. *New J. Phys.* **18**, 115001 (2016).

40. Douglas, S. M. *et al.* Self-assembly of DNA into nanoscale three-dimensional shapes. *Nature* **459**, 414–418 (2009).

41. Sprengel, A. *et al.* Tailored protein encapsulation into a DNA host using geometrically organized supramolecular interactions. *Nat. Commun.* **8**, 14472 (2017).

42. Aghebat Rafat, A., Sagredo, S., Thalhammer, M. & Simmel, F. C. Barcoded DNA origami structures for multiplexed optimization and enrichment of DNA-based protein-binding cavities. *Nat. Chem.* **12**, 852–859 (2020).